# Mechanism of Dihydroneopterin Aldolase: Functional Roles of the Conserved Active Site Glutamate and Lysine Residues†

Yi Wang, Yue Li, and Honggao Yan*

*Department of Biochemistry and Molecular Biology, Michigan State University, East Lansing, Michigan 48824*

*Received May 12, 2006; Revised Manuscript Received August 23, 2006*

ABSTRACT: Dihydroneopterin aldolase (DHNA) catalyzes the conversion of 7,8-dihydroneopterin (DHNP) to 6-hydroxymethyl-7,8-dihydropterin (HP) in the folate biosynthetic pathway. There are four conserved active site residues at the active site, E22, Y54, E74, and K100 in *Staphylococcus aureus* DHNA (SaDHNA), corresponding to E21, Y53, E73, and K98, respectively, in *Escherichia coli* DHNA (EcDHNA). The functional roles of the conserved glutamate and lysine residues have been investigated by site-directed mutagenesis in this work. E22 and E74 of SaDHNA and E21, E73, and K98 of EcDHNA were replaced with alanine. K100 of SaDHNA was replaced with alanine and glutamine. The mutant proteins were characterized by equilibrium binding, stopped-flow binding, and steady-state kinetic analyses. For SaDHNA, none of the mutations except E74A caused dramatic changes in the affinities of the enzyme for the substrate or product analogues or the rate constants. The $K_d$ values for SaE74A were estimated to be $>3000$ $\mu$M, suggesting that the $K_d$ values of the mutant are at least 100 times those of the wild-type enzyme. For EcDHNA, the E73A mutation increased the $K_d$ values for the substrate or product analogues neopterin (MP), monapterin (NP), and 6-hydroxypterin (HPO) by factors of 340, 160, and 5600, respectively, relative to those of the wild-type enzyme. The K98A mutation increased the $K_d$ values for NP, MP, and HPO by factors of 14, 3.6, and 230, respectively. The E21A mutation increased the $K_d$ values for NP and HPO by factors of 2.2 and 42, respectively, but decreased the $K_d$ value for MP by a factor of 3.3. The E22 (E21) and K100 (K98) mutations decreased the $k_{cat}$ values by factors of $1.3-2 \times 10^4$. The E74 (E73) mutation decreased in the $k_{cat}$ values by factors of $\sim$10. The results suggested that E74 of SaDHNA and E73 of EcDHNA are important for substrate binding, but their roles in catalysis are minor. In contrast, E22 and K100 of SaDHNA are important for catalysis, but their roles in substrate binding are minor. On the other hand, E21 and K98 of EcDHNA are important for both substrate binding and catalysis.

Dihydroneopterin aldolase (DHNA)[1] catalyzes the conversion of the 7,8-dihydroneopterin (DHNP) to 6-hydroxymethyl-7,8-dihydropterin (HP) in the folate biosynthetic pathway, one of the principal targets for developing antimicrobial agents (*1*−*3*). Folate cofactors are essential for life (*4*). Most microorganisms must synthesize folates de novo. In contrast, mammals cannot synthesize folates because of the lack of three enzymes in the middle of the folate pathway and obtain folates from the diet. DHNA is the first of the three enzymes that are absent in mammals and therefore an attractive target for the development of antimicrobial agents (*5*).

DHNA is a unique aldolase in two respects. First, DHNA requires neither the formation of a Schiff base between the substrate and enzyme nor metal ions for catalysis (*6*). Aldolases can be divided into two classes based on their catalytic mechanisms (*7*, *8*). Class I aldolases require the formation of a Schiff base between an amino group of the enzyme and the carbonyl of the substrate, whereas class II aldolases require a $Zn^{2+}$ ion at their active sites for catalysis. The proposed catalytic mechanism for DHNA is similar to that of class I aldolases, but the Schiff base is embedded in the substrate. Second, in addition to the aldolase reaction, DHNA also catalyzes the epimerization at the 2′-carbon of DHNP to generate 7,8-dihydromonapterin (DHMP) (Figure 1A) (*9*), but the biological function of the epimerase reaction is not known at present. Interestingly, DHNAs from *Staphylococcus aureus* (SaDHNA) and *Escherichia coli* (EcDHNA) have significant differences in their binding and catalytic properties (Y. Wang et al., unpublished results).

DHNA consists of eight identical subunits. The atomic structures of SaDHNA (*5*, *10*), *Mycobacterium tuberculosis* DHNA (*11*), and *Arabidopsis thaliana* DHNA (*12*) have been determined by X-ray crystallography. The octameric structures look like two stacked donuts with a large hole in the middle, $\sim$13 Å in SaDHNA. Each donut consists of four subunits. There are eight active sites, all formed by residues from two adjacent subunits. At the active sites, there are four conserved residues that interact with the bound product HP

† This work was supported in part by NIH Grant GM51901 (H.Y.).

* To whom correspondence should be addressed. Telephone: (517) 353-5282. Fax: (517) 353-9334. E-mail: yanh@msu.edu.

[1] Abbreviations: DHMP, 7,8-dihydro-L-monapterin; DHNA, dihydroneopterin aldolase; DHNP, 7,8-dihydro-D-neopterin; EcDHNA, *E. coli* dihydroneopterin aldolase; EcE21A, EcDHNA with E21 replaced with alanine; EcE73A, EcDHNA with E73 replaced with alanine; EcK98A, EcDHNA with K98 replaced with alanine; HP, 6-hydroxymethyl-7,8-dihydropterin; HPO, 6-hydroxymethyl-7,8-dihydropterin; MP, L-monapterin; NP, D-neopterin; SaDHNA, *S. aureus* dihydroneopterin aldolase; SaE22A, SaDHNA with E22 replaced with alanine; SaE74A, SaDHNA with E74 replaced with alanine; SaK100A, SaDHNA with K100 replaced with alanine; SaK100Q, SaDHNA with K100 replaced with glutamine.

10.1021/bi060949j CCC: $33.50 
Published on Web 12/19/2006

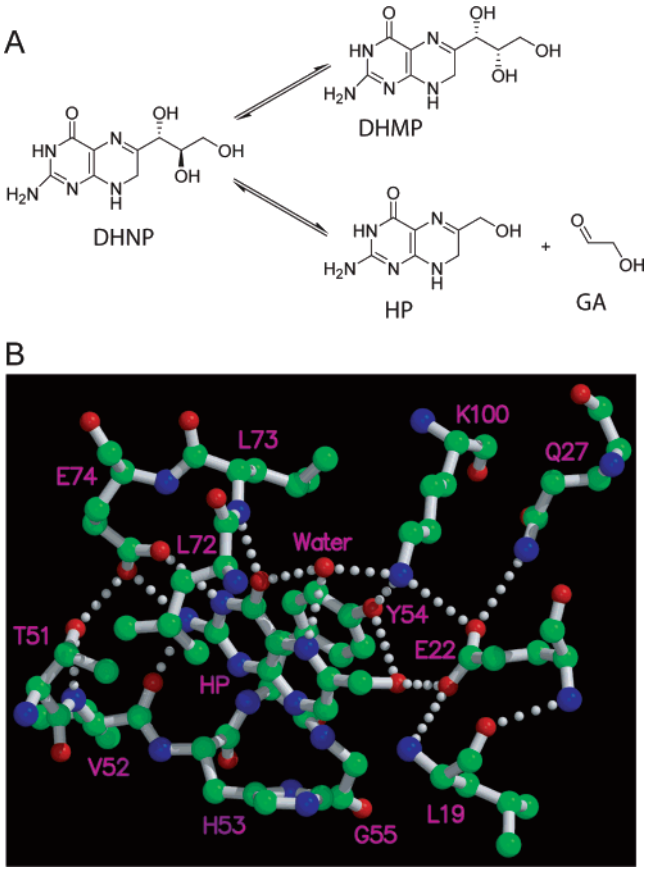


FIGURE 1: Reactions catalyzed by DHNA (A) and the interactions of HP with SaDHNA (B). The interactions between HP and SaDHNA are drawn on the basis of the crystal structure of SaDHNA in complex with HP (*10*). The hydrogen bonds are drawn as dotted lines. Oxygen atoms are colored red, nitrogen atoms blue, and carbon atoms green. Panel B was prepared with the programs Molscript (*20*) and Raster3D (*21*, *22*).

as revealed by the crystal structures (*10*, *11*) (Figure 1B). These four residues are E22, Y54, E74, and K100 in SaDHNA, corresponding to E21, Y53, E73, and K98, respectively, in EcDHNA (Figure 2). Previously, we showed that the conserved tyrosine residue plays a critical role in DHNA catalysis (*13*). Substitution of the conserved tyrosine residue in SaDHNA or EcDHNA with phenylalanine turned the target enzyme into an oxygenase. In this paper, we describe a site-directed mutagenesis study of the functional roles of the other conserved, active site residues in SaDHNA and EcDHNA. The results provide important insight into the catalytic mechanisms of the enzymes and valuable information for designing inhibitors targeting these enzymes.

## EXPERIMENTAL PROCEDURES

*Materials.* 6-Hydroxymethylpterin (HPO), 6-hydroxymethyl-7,8-dihydropterin (HP), 7,8-dihydro-D-neopterin (DHNP), 7,8-dihydro-L-monapterin (DHMP), D-neopterin (NP), and L-monapterin (MP) were purchased from Schircks Laboratories. *pfu* DNA polymerase was purchased from Strategene. Other chemicals were from Sigma or Aldrich.

*Site-Directed Mutagenesis and Protein Purification*. The site-directed mutants were made by a PCR-based method using high-fidelity *pfu* DNA polymerase according to a protocol developed by Stratagene. The forward and reverse primers for the PCR-based mutagenesis experiments are listed in Table 1. The mutants were selected by DNA sequencing. To ensure that there were no unintended mutations in the mutants, the entire coding sequences of the mutated genes were determined. The *S. aureus* enzymes contained seven extra residues (MHHHHHH) at the N-terminus serving as a His tag for purification.

EcE21A, EcE73A, and EcK98A, which were mutants of EcDHNA with E21, E73, and K98 replaced with alanine, respectively, were purified with a DEAE-cellulose column followed by a Bio-Gel A-0.5m gel column. Briefly, the *E. coli* cells were resuspended in 20 mM Tris-HCl (pH 8.0) (buffer A) and lysed with a French press. The lysate was centrifuged for 20 min at ~27000*g*. The supernatant was loaded onto a DEAE-cellulose column equilibrated with buffer A. The column was washed with buffer A until the $OD_{280}$ of the effluent was <0.05 and eluted with a 0 to 500 mM linear NaCl gradient in buffer A. Fractions containing DHNA were identified by $OD_{280}$ and SDS−PAGE and concentrated to ~15 mL with an Amicon concentrator using a YM30 membrane. The concentrated protein solution was centrifuged, and the supernatant was applied to a Bio-Gel A-0.5m gel column equilibrated with buffer A containing 150 mM NaCl. The column was developed with the same buffer. Fractions from the gel filtration column were monitored by $OD_{280}$ and SDS−PAGE. Pure DHNA fractions were pooled and concentrated to 10−20 mL. The concentrated DHNA was dialyzed against 5 mM Tris-HCl (pH 8.0), lyophilized, and stored at −80 °C.

SaE22A, SaE74A, SaK100A, and SaK100Q, which were mutants of SaDHNA, were purified to homogeneity with a Ni-NTA column followed by a Bio-Gel A-0.5m gel column. Briefly, the cells were harvested and lysed as described above except that buffer was replaced with 50 mM sodium phosphate, 300 mM NaCl (pH 8.0) (buffer B), and 10 mM imidazole. The lysate was loaded onto the Ni-NTA column equilibrated with buffer B containing 10 mM imidazole. The column was washed with 20 mM imidazole in buffer B and eluted with 250 mM imidazole in buffer B. The concentrated protein was further purified by gel filtration, concentrated again, dialyzed, lyophilized, and stored at −80 °C as described earlier.

*Equilibrium Binding Studies.* The procedures for the equilibrium binding studies of DHNAs were essentially the same as those previously described for the similar studies of 6-hydroxymethyl-7,8-dihydropterin pyrophosphokinase using a Spex FluoroMax-2 fluorometer (*14*, *15*). Briefly, proteins and ligands were all dissolved in 100 mM Tris-HCl (pH 8.3), and the titration experiments were performed in a single cuvette at 24 °C. The equilibrium binding experiments were performed by titrating either ligands or the proteins. In ligand titrations, fluorescence intensities were measured at an emission wavelength of 446 nm with a slit of 5 nm. The excitation wavelength and slit were 400 and 1 nm, respectively. A set of control data was obtained in the absence of the protein. The data set obtained in the absence of the protein was then subtracted from the corresponding data set obtained in the presence of the protein after correcting inner filter effects. The $K_d$ value was obtained by nonlinear least-squares fitting of the titration data as previously described (*14*). All $K_d$ values for SaDHNA mutants except that of SaE22A for HPO were obtained by titrating ligands.

```
         10        20        30        40        50
MQDTIFLKGMRFYGYHGALSAENEIGQIFKVDVTLKVDLAEAGRTDNVID
 MDIVFIEQLSVITTIGVYDWEQTIEQKLVFDIEMAWDNRKAAKSDDVAD
         10        20        30        40

         60        70        80        90       100
TVHYGEVFEEVKSIMEGKAVNLLEHLAERIANRINSQYNRVMETKVRITK
CLSYADIAETVVSHVEGARFALVERVAEEVAELLLARFNS-PWVRIKLSK
         60        70        80        90

       110
ENPPIPGHYDGVGIEIVRENK
PGA-VA-RAANVGVIIERGNNLKENN
          110
```

FIGURE 2: Amino acid sequence alignment of SaDHNA and EcDHNA. The amino acid sequence of EcDHNA is aligned with that of SaDHNA with gaps inserted on the basis of the crystal structure of SaDHNA. Residue numbering for SaDHNA is above the amino acid sequence, and that for EcDHNA is below the amino acid sequence. The strictly conserved residues, on the basis of the sequence alignment of 67 DHNAs (not shown), are highlighted in bold.

Table 1: Forward and Reverse Primers for the PCR-Based Mutagenesis Experiments

| mutant | primer[a] |
|---|---|
| SaE22A | 5′-GGTGCTTTATCAGCTGCAAATGAAATAGGGCAAATTTTC-3′ |
| | 5′-GAAAATTTGCCCTATTTCATTTGCAGCTGATAAAGCACC-3′ |
| SaE74A | 5′-GCCGTTAATTTACTTGCGCATCTAGCTGAACGTATTGC-3′ |
| | 5′-GCAATACGTTCAGCTAGATGCGCAAGTAAATTAACGGC-3′ |
| SaK100A | 5′-GAAACGAAAGTGAGAATCACTGCAGAAAACCCACCGATTCCG-3′ |
| | 5′-CGGAATCGGTGGGTTTTCTGCAGTGATTCTCACTTTCGTTTC-3′ |
| SaK100Q | 5′-CGAAAGTGAGAATCACTCAAGAAAACCCACCGATTCC-3′ |
| | 5′-GGAATCGGTGGGTTTTCTTGAGTGATTCTCACTTTCG-3′ |
| EcE21A | 5′-GTGTTTACGACTGGGCACAGACCATCGAACAG-3′ |
| | 5′-CTGTTCGATGGTCTGTGCCCAGTCGTAAACAC-3′ |
| EcE73A | 5′-GCGCTGGTGGCACGCGTGGCTG-3′ |
| | 5′-CAGCCACGCGTGCCACCAGCGC-3′ |
| EcK98A | 5′-CGTATCAAACTCAGCGCGCCAGGCGCAGTGG-3′ |
| | 5′-CCACTGCGCCTGGCGCGCTGAGTTTGATACG-3′ |

[a] The forward primers are listed first with the mutations underlined. The mutations in the reverse primers are not indicated.

In protein titration experiments, a ligand solution was titrated with a stock solution of one of the mutant proteins. Fluorescence intensities were measured at an emission wavelength of 430 nm and an excitation wavelength of 330 nm. The emission and excitation slits were both 5 nm. A control titration experiment was performed in the absence of the ligand. The control data set obtained in the absence of HP was subtracted from the corresponding data set obtained in the presence of the ligand. The $K_d$ value was obtained by nonlinear least-squares fitting of the titration data as previously described (*14*). All $K_d$ values for EcDHNA mutants and that of SaE22A for HPO were obtained by titrating proteins.

*Stopped-Flow Analysis*. Stopped-flow experiments were performed on an Applied Photophysics SX.18MV-R stopped-flow spectrofluorometer at 25 °C. One syringe contained one of the mutant proteins, and the other contained NP, MP, HP, or HPO. The protein concentrations were 1 or 2 $\mu$M, and the ligand concentrations ranged from 5 to 60 $\mu$M. All concentrations were those after the mixing of the two syringe solutions. Fluorescence traces for NP, MP, and HPO were obtained with an excitation wavelength of 360 nm and a filter with a cutoff of 395 nm for emission. Fluorescence traces for HP were obtained with an excitation wavelength of 330 nm and the same filter for emission. Apparent rate constants were obtained by nonlinear leats-squares fitting of the data to a single-exponential equation and were replotted against the ligand concentrations. The association and dissociation rate constants were obtained by linear regression of the apparent rate constants versus ligand concentration data.

*Steady-State Kinetic Assay.* All components were dissolved in a buffer containing 100 mM Tris-HCl, 1 mM EDTA, and 5 mM DTT (pH 8.3). The reactions were initiated by mixing with the mutant enzymes and quenched with 1 N HCl. The quenched reaction mixtures were processed as previously described (*9*). Briefly, the reaction mixtures (115 $\mu$L each) were mixed with 50 $\mu$L of 1% (w/v) $I_2$ and 2% (w/v) KI in 1 N HCl for 5 min at room temperature to oxidize the pterin compounds. Excess iodine was reduced by mixing the samples with 25 $\mu$L of 2% (w/v) ascorbic acid. The samples were then centrifuged at room temperature for 5 min using a microcentrifuge. The oxidized reactant and products in the supernatants were separated by HPLC using a Vydac RP18 column. The column was equilibrated with 20 mM $NaH_2PO_4$ made with MilliQ water and eluted at a flow rate of 0.8 mL/min with the same solution. The oxidized reactant and products were quantified by on-line fluorometry with excitation and emission wavelengths of 365 and 446 nm, respectively. High concentrations of the mutant enzymes, ranging from 1 to 20 $\mu$M, were used in the kinetic assays because of their low activities. When the substrate concentrations were in large excess of the enzyme, the normal Michaelis−Menten equation was used to obtain kinetic constants by nonlinear least-squares regression. When the enzyme concentration was comparable to the substrate concentrations because of the extremely low activity of the

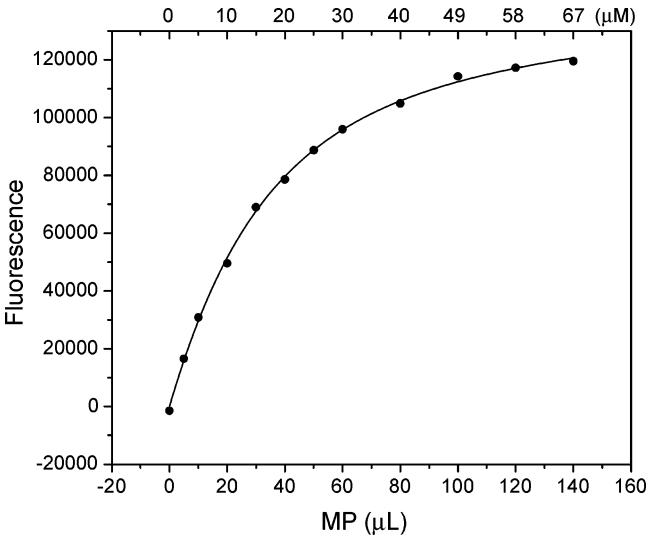


FIGURE 3: Binding of MP to SaE22A at equilibrium. A 2 mL solution containing 10 $\mu$M SaE22A in 100 mM Tris-HCl (pH 8.3) was titrated with MP by adding aliquots of a 1.03 mM MP stock solution at 24 °C. The final enzyme concentration was 9.3 $\mu$M. The top axis indicates the MP concentrations during the titration. A set of control data was obtained in the absence of the enzyme and was subtracted from the corresponding data set obtained in the presence of the enzyme. The solid line was obtained by nonlinear least-squares regression as previously described (*14*).

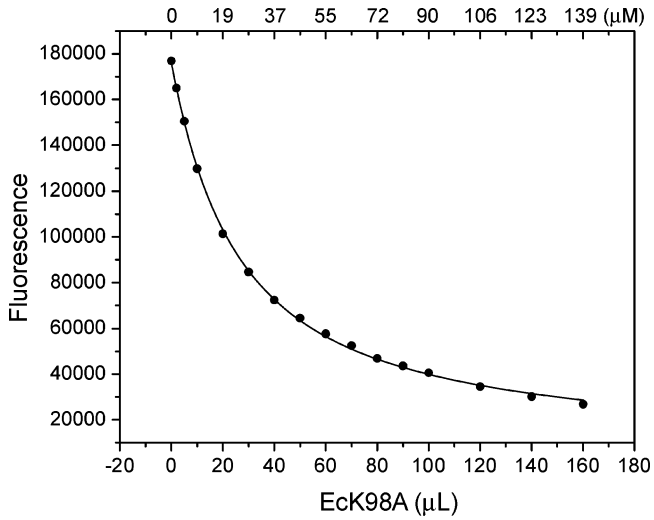


FIGURE 4: Binding of HPO to EcK98A at equilibrium. A 2 mL solution containing 5 $\mu$M HPO in 100 mM Tris-HCl (pH 8.3) was titrated with EcK98A by adding aliquots of a 1.9 mM EcK98A stock solution at 24 °C. The final HPO concentration was 4.6 $\mu$M. The top axis indicates the EcK98A concentrations during the titration. A set of control data was obtained in the absence of HPO and was subtracted from the corresponding data set obtained in the presence of HPO. The solid line was obtained by nonlinear least-squares regression as previously described (*14*).

enzyme, a modified steady-state kinetic equation (eq 1) (*16*) was used to evaluate kinetic constants.

$$v = \frac{k_{cat}}{2}[E_t + S_t + K_m - \sqrt{(E_t + S_t + K_m)^2 - 4E_tS_t}] \quad (1)$$

where $E_t$ and $S_t$ are the total enzyme and substrate concentrations, respectively, and $k_{cat}$ and $K_m$ have the usual meanings.

## RESULTS

*Binding Studies*. Previously, we established the thermodynamic and kinetic framework for the structure−function studies of SaDHNA and EcDHNA by equilibrium measurements and stopped-flow and quench-flow analyses (Y. Wang et al., unpublished results). A similar strategy was used for the characterization of the site-directed mutants. The binding steps were mimicked with the substrate and product analogues NP, MP, and HPO. The difference between the substrate and product analogues and the corresponding substrate and products is that between C7 and N8 there is a double bond in the analogues and a single bond in the substrate and products. NP, MP, and HPO are excellent substrate and product analogues for the study of binding steps for two reasons. (i) According to the crystal structure of the complex of SaDHNA and HP (*10*), there is no hydrogen bond between N7 of HP and the protein. By implication, there may not be a hydrogen bond between N7 of DHNP or DHMP and the protein. Therefore, the reduced and oxidized pterins may have similar affinities for the enzymes. (ii) Indeed, HP and HPO have similar affinities for the enzymes (Y. Wang et al., unpublished results). The $K_d$ values were measured by equilibrium binding experiments using fluorometry by either titrating the ligands or the proteins. Representative results of the equilibrium binding studies are shown in Figures 3 and 4. The association and dissociation rate constants were determined by kinetic binding experiments using stopped-flow fluorometry. A representative result of the kinetic binding studies is shown in Figure 5. For technical reasons, the binding constants for SaE74A and the association and dissociation rate constants for EcE73A could not be measured. The complete results of the binding studies are summarized in Tables 2 and 3 for SaDHNA and EcDHNA, respectively. In general, the thermodynamic data are in good agreement with the kinetic data, as the measured $K_d$ values are in good agreement with those calculated from the association and dissociation rate constants. High $K_d$ values are, for the most part, due to high dissociation rate constants. For SaDHNA, none of the mutations except E74A caused dramatic changes in the affinities of the enzyme for the substrate or product analogues or the rate constants. The $K_d$ values for SaE74A were estimated to be $>3000$ $\mu$M, suggesting that the $K_d$ values of the mutant are at least 100 times greater than those of the wild-type enzyme. The results indicated that for SaDHNA, of the three conserved residues, only E74 is important for the binding of the analogues. For EcDHNA, similarly, the mutation of E73, corresponding to E74 in SaDHNA, had the most dramatic effects on ligand binding. The E73A mutation increased the $K_d$ values for the binding of NP, MP, and HPO by factors of 340, 160, and 5600, respectively, relative to those of the wild-type enzyme, suggesting that E73 is critically important for the binding of these substrate or product analogues. In addition, the K98A mutation increased the $K_d$ values for the binding of NP, MP, and HPO by factors of 14, 3.6, and 230, respectively, suggesting that K98 is important for the binding of these ligands, particularly for the binding of HPO and NP. The E21A mutation increased the $K_d$ values for the binding of NP and HPO by factors of 2.2 and 42, respectively, but decreased the $K_d$ value for the binding of MP by a factor of 3.3, suggesting that E21 is only important for the binding of HPO.

*Steady-State Kinetic Studies*. The catalytic properties of the mutants were determined by steady-state kinetic mea-

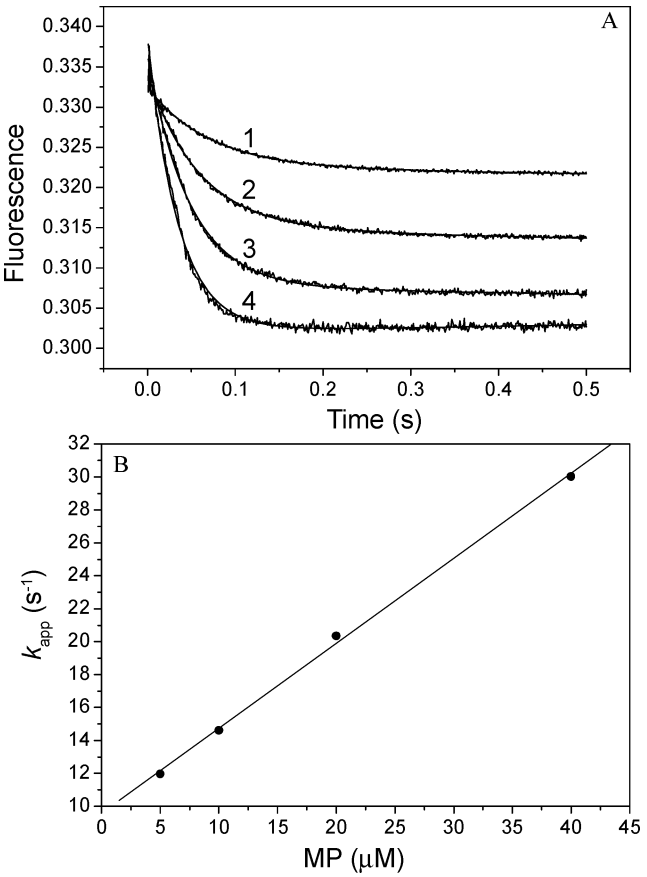


FIGURE 5: Stopped-flow fluorometric analysis of the binding of HPO to SaE22A. The concentration of SaE22A was 1 $\mu$M, and the concentrations of HPO were 5, 10, 20, and 40 $\mu$M for traces 1−4, respectively. All concentrations were those immediately after the mixing of the two syringe solutions. Both SaE22A and HPO were dissolved in 100 mM Tris-HCl (pH 8.3). The fluorescent signals were rescaled so that they could be fitted into the figure with clarity. The solid lines were obtained by nonlinear regression as described in Experimental Procedures. Panel B is a replot of the apparent rate constants vs the HPO concentrations. The solid line was obtained by linear regression.

surements. Because the reactions were slow, no quench-flow apparatus was needed. For technical reasons, mainly because of the solubility limits of DHNP and DHMP, only $k_{cat}/K_m$ could be estimated for SaF74A. Also, only $k_{cat}$ could be estimated for SaK100Q, because the fluorescence of some unknown small molecules associated with the protein preparation caused significant errors in the reaction rates at low substrate concentrations. The steady-state kinetic parameters of the SaDHNA and EcDHNA mutants are summarized in Tables 4 and 5, respectively. For SaDHNA, the E22A mutation decreased the $k_{cat}$ by a factor of $4.8 \times 10^3$ with DHNP as the substrate and $1.5 \times 10^3$ with DHMP as the substrate, in comparison with those of the wild-type enzyme. The K100A and K100Q mutations decreased $k_{cat}$ values by factors of $2 \times 10^4$ and $2.8 \times 10^3$, respectively, with DHNP as the substrate and by factors of $2 \times 10^3$ and $1.8 \times 10^3$, respectively, with DHMP as the substrate. The effects of the two mutations were very similar. The results suggest that both E22 and K100 are important for catalysis. The $k_{cat}$ value of SaE74A mutant could not be determined, but its $k_{cat}/K_m$ value could be estimated from the linear part of the reaction rate versus substrate concentration curve, which decreased by a factor of 570 with DHNP as the substrate and a factor of 23 with DHMP as the substrate. The decreases in the $k_{cat}/K_m$ values are probably largely due to the increases in $K_m$, considering that the mutation caused dramatic decreases in the affinities of the enzyme for all substrate or product analogues. The result suggests that E74 plays no great role in catalysis. This was confirmed by the mutation of the corresponding residue (E73) of EcDHNA. The E73A mutation of EcDHNA caused a decrease in $k_{cat}$ by a factor of only ~10. The EcE21A and EcK98A mutants behaved like the corresponding SaDHNA mutants (SaE22A and SaK100A) in terms of their $k_{cat}$ values. Thus, the $k_{cat}$ of EcE21A decreased by a factor of $1.3 \times 10^3$ with DHNP as the substrate and by a factor of $3.9 \times 10^3$ with DHMP as the substrate, in comparison with those of the wild-type *E. coli* enzyme. The $k_{cat}$ of EcK98A decreased by a factor of $1.9 \times 10^4$ with DHNP as the substrate and by a factor of $1.7 \times 10^4$ with DHMP as the substrate. The results suggest that the conserved glutamate and lysine residues both are important as well for the catalysis by EcDHNA.

## DISCUSSION

Figure 6 illustrates the proposed chemical mechanism for the DHNA-catalyzed reaction (*6*, *9*, *10*). The epimerization reaction is proposed to occur via the intermediate for the retroaldol reaction. However, little is known about how DHNA catalyzes the reaction.

Of the published crystal structures of DHNAs (*5*, *10*−*12*), the most informative structures are the binary HP complexes of SaDHNA and *M. tuberculosis* DHNA, which reveal the atomic interactions between the pterin moiety of the substrate and the enzymes. Four conserved residues and an important water molecule are found at the active site, as illustrated in Figure 1B for SaDHNA. The structure of SaDHNA in complex with the substrate analogue NP (*5*) should provide the structural information about the interaction between the trihydroxypropyl moiety and the enzyme. Unfortunately, the occupancy value is 0 with an *R* factor of 100 for all trihydroxypropyl atoms of the bound NP, suggesting that the trihydroxypropyl moiety of NP was not seen in the crystal and no structural information about the interaction between the trihydroxypropyl moiety and the enzyme can be deduced from the crystal structure.

The interactions between pterin and DHNA are reminiscent of those of dihydrofolate reductase (DHFR) with dihydrofolate, which also contains a pterin moiety. The common features include two hydrogen bonds between a carboxylate group of a glutamate or aspartate and the 2-$NH_2$ and 3-NH groups of the pterin and a hydrogen bond between a water molecule and N5 of the pterin. Replacement of D27 of *E. coli* DHFR, a residue corresponding to E74 of SaDHNA and E73 of EcDHNA, with asparagine or serine causes a significant decrease in $k_{cat}$ and a significant increase in $K_m$ or $K_d$, suggesting that the aspartate is important for both substrate binding and catalysis (*17*). On the other hand, replacement of D26 of *Lactobacillus casei* DHFR, which corresponds to D27 of *E. coli* DHFR, with asparagine causes a <10-fold decrease in $k_{cat}$ and essentially no change in $K_m$ or $K_d$, suggesting that the carboxyl group is not important for substrate binding but may play a minor role in catalysis (*18*). For DHNA, the biochemical properties of SaE74A and EcE73A indicate that the conserved glutamate is very

Table 2: Binding Constants of SaDHNA and Site-Directed Mutants[a]

| | | SaDHNA | SaE22A | SaE74A | SaK100A | SaK100Q |
|---|---|---|---|---|---|---|
| NP | $K_d$ ($\mu$M) | 18 ± 2 | 13 ± 0.6 | >4000 | 6.9 ± 0.7 | 11 ± 0.3 |
| | $k_1$ ($M^{-1}$ $s^{-1}$) | (2.4 ± 0.1) × $10^5$ | (2.9 ± 0.1) × $10^5$ | nd[b] | (2.2 ± 0.1) × $10^5$ | (1.9 ± 0.1) × $10^5$ |
| | $k_{-1}$ ($s^{-1}$) | 4.5 ± 0.1 | 4.0 ± 0.1 | nd[b] | 1.2 ± 0.1 | 2.0 ± 0.1 |
| MP | $K_d$ ($\mu$M) | 13 ± 1 | 11 ± 0.9 | >3000 | 9.1 ± 0.6 | 13 ± 1 |
| | $k_1$ ($M^{-1}$ $s^{-1}$) | (2.9 ± 0.2) × $10^5$ | (3.1 ± 0.1) × $10^5$ | nd[b] | (2.7 ± 0.1) × $10^5$ | (2.8 ± 0.1) × $10^5$ |
| | $k_{-1}$ ($s^{-1}$) | 4.2 ± 0.2 | 4.0 ± 0.1 | nd[b] | 2.1 ± 0.1 | 4.3 ± 0.1 |
| HPO | $K_d$ ($\mu$M) | 24 ± 0.2 | 17 ± 2 | >6000 | 6.0 ± 0.1 | 8.8 ± 0.4 |
| | $k_1$ ($M^{-1}$ $s^{-1}$) | (4.5 ± 0.2) × $10^5$ | (5.6 ± 0.3) × $10^5$ | nd[b] | (6.4 ± 0.3) × $10^5$ | (6.8 ± 0.4) × $10^5$ |
| | $k_{-1}$ ($s^{-1}$) | 10 ± 0.5 | 10 ± 0.2 | nd[b] | 5.8 ± 0.3 | 5.8 ± 0.1 |

[a] Both wild-type SaDHNA and mutants have a His tag (MHHHHHH) at the N-terminus. We have shown previously that the His tag has no effects on the binding and catalytic properties of the enzyme. The chemical structures of the measured compounds are as follows.

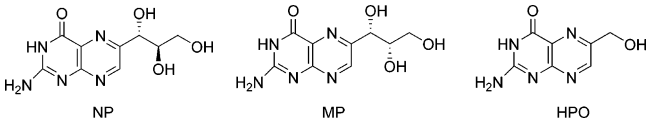


[b] Not determined.

Table 3: Binding Constants of EcDHNA and Site-Directed Mutants

| | | EcDHNA | EcE21A | EcE73A | EcK98A |
|---|---|---|---|---|---|
| NP | $K_d$ ($\mu$M) | 0.77 ± 0.06 | 1.7 ± 0.01 | 260 ± 40 | 11 ± 0.3 |
| | $k_1$ ($M^{-1}$ $s^{-1}$) | (3.2 ± 0.2) × $10^5$ | (4.6 ± 0.2) × $10^5$ | nd[a] | (6.6 ± 0.1) × $10^5$ |
| | $k_{-1}$ ($s^{-1}$) | 0.29 ± 0.03 | 0.82 ± 0.02 | nd[a] | 7.2 ± 0.3 |
| MP | $K_d$ ($\mu$M) | 2.6 ± 0.06 | 0.80 ± 0.01 | 420 ± 20 | 9.4 ± 0.09 |
| | $k_1$ ($M^{-1}$ $s^{-1}$) | (2.6 ± 0.1) × $10^5$ | (4.3 ± 0.2) × $10^5$ | nd[a] | (9.1 ± 0.4) × $10^5$ |
| | $k_{-1}$ ($s^{-1}$) | 0.58 ± 0.03 | 0.47 ± 0.02 | nd[a] | 9.1 ± 0.6 |
| HPO | $K_d$ ($\mu$M) | 0.10 ± 0.007 | 4.2 ± 0.01 | 560 ± 20 | 23 ± 2 |
| | $k_1$ ($M^{-1}$ $s^{-1}$) | (5.5 ± 0.4) × $10^5$ | (1.4 ± 0.1) × $10^6$ | nd[a] | (1.2 ± 0.1) × $10^6$ |
| | $k_{-1}$ ($s^{-1}$) | 0.062 ± 0.006 | 6.3 ± 0.2 | nd[a] | 27 ± 1 |

[a] Not determined.

Table 4: Steady-State Kinetic Constants of SaDHNA and Site-Directed Mutants

| | | SaDHNA | SaE22A | SaE74A | SaK100A | SaK100Q |
|---|---|---|---|---|---|---|
| DHNP | $k_{cat}$ ($s^{-1}$) | 0.045 ± 0.002 | (9.3 ± 0.4) × $10^{-6}$ | nd[a] | (2.2 ± 0.1) × $10^{-6}$ | (1.6 ± 0.3) × $10^{-5}$ |
| | $K_m$ ($\mu$M) | 4.6 ± 0.3 | 3.9 ± 0.6 | nd[a] | 5.8 ± 1 | nd[a] |
| | $k_{cat}/K_m$ ($s^{-1}$ $M^{-1}$) | 9.7 | 2.4 × $10^{-3}$ | (1.7 ± 0.09) × $10^{-2}$ | 3.7 × $10^{-4}$ | |
| DHMP | $k_{cat}$ ($s^{-1}$) | 0.01 ± 0.001 | (6.5 ± 0.2) × $10^{-6}$ | nd[a] | (5.1 ± 0.1) × $10^{-6}$ | (5.7 ± 0.9) × $10^{-6}$ |
| | $K_m$ ($\mu$M) | 5.5 ± 0.2 | 4.0 ± 0.6 | nd[a] | 9.5 ± 0.7 | nd[a] |
| | $k_{cat}/K_m$ ($s^{-1}$ $M^{-1}$) | 1.8 | 1.6 × $10^{-3}$ | (8.0 ± 0.08) × $10^{-2}$ | 5.4 × $10^{-4}$ | |

[a] Not determined.

Table 5: Steady-State Kinetic Constants of EcDHNA and Site-Directed Mutants

| | | EcDHNA | EcE21A | EcE73A | EcK98A |
|---|---|---|---|---|---|
| DHNP | $k_{cat}$ ($s^{-1}$) | 0.082 ± 0.001 | (6.5 ± 0.3) × $10^{-5}$ | (7.3 ± 0.6) × $10^{-3}$ | (4.3 ± 0.03) × $10^{-6}$ |
| | $K_m$ ($\mu$M) | 7.4 ± 0.3 | 1.6 ± 0.3 | 9700 ± 1000 | 2.4 ± 0.1 |
| | $k_{cat}/K_m$ ($s^{-1}$ $M^{-1}$) | 11 | 4.2 × $10^{-2}$ | 7.6 × $10^{-4}$ | 1.8 × $10^{-3}$ |
| DHMP | $k_{cat}$ ($s^{-1}$) | 0.089 ± 0.004 | (2.3 ± 0.2) × $10^{-5}$ | (6.0 ± 1) × $10^{-3}$ | (5.3 ± 0.05) × $10^{-6}$ |
| | $K_m$ ($\mu$M) | 8.0 ± 0.6 | 0.76 ± 0.2 | 9800 ± 3000 | 2.9 ± 0.2 |
| | $k_{cat}/K_m$ ($s^{-1}$ $\mu M^{-1}$) | 11 | 3.1 × $10^{-2}$ | 6.1 × $10^{-4}$ | 1.8 × $10^{-3}$ |

important for substrate binding and its role in catalysis is a minor one if any. It contributes to the binding of the pterin compounds by 3−5 kcal/mol on the basis of the binding data of the two mutants.

The hallmark of the DHNA-catalyzed reaction is general acid and base catalysis (Figure 6). The formation of the intermediate of the retroaldol reaction requires the protonation of N5 and the deprotonation of the 2′-OH group of DHNP. The formation of HP requires the deprotonation of 5-NH and the protonation of the enol group of the reaction intermediate. The epimerization reaction is essentially the reversal of the chemical step for the formation of the reaction intermediate following the flip of GA. We have recently shown that the conserved active site tyrosine residue, corresponding to Y54 in SaDHNA and Y53 in EcDHNA, plays an important role in the protonation of the enol group of the reaction intermediate to form HP (*13*). Replacement of either Y54 of SaDHNA or Y53 of EcDHNA causes a dramatic decrease in the rate for the formation of HP but no significant change in the rate for the formation of the reaction intermediate. Either mutation converts the aldolase to an oxygenase. The water molecule that is hydrogen bonded to N5 of HP in the crystal structures (*10*, *11*) is most likely the general acid for the protonation of N5 of DHNP and its

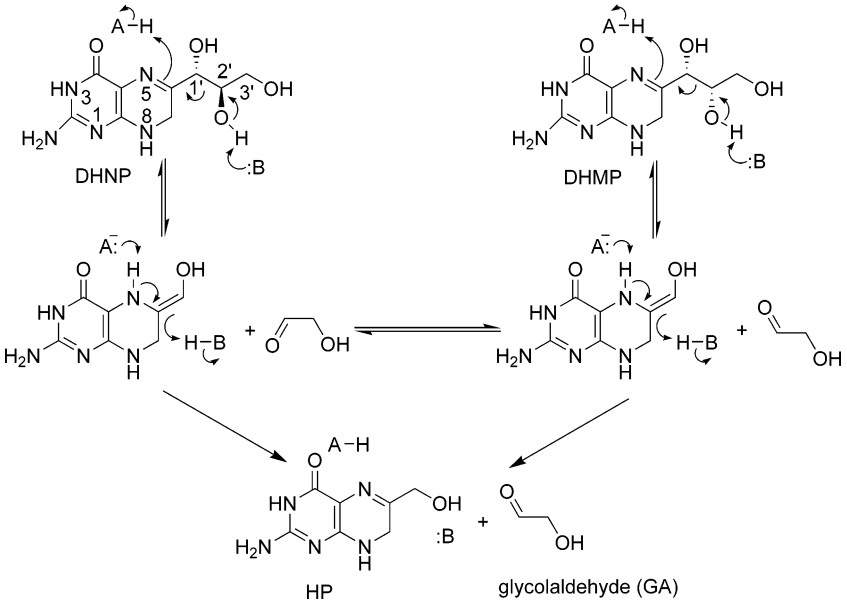


FIGURE 6: Proposed catalytic mechanism for the DHNA-catalyzed reactions.

conjugated base for the deprotonation of the 5-NH group of the reaction intermediate, because no amino acid residue is in a position to play such a role according to the crystal structures. There are several candidate residues that may act as a general base for the deprotonation of the 2′-OH group of DHNP according to the crystal structures, including E22, Y54, and K100 (SaDHNA numbering). Y54 can be excluded on the basis of our previous site-directed mutagenesis of the conserved tyrosine residue (*13*). The site-directed mutagenesis study presented here suggests that both E22 and K100 are important for catalysis, with K100 contributing a bit more to the transition-state stabilization. The larger contribution by K100 is probably due to its hydrogen bond with the water molecule that serves as a general acid in the first chemical step of the enzymatic reaction. However, from the chemical perspective, K100 is much more likely to serve as a general base for the deprotonation of the 2′-OH group of DHNP. The optimal pH for the DHNA-catalyzed reaction is 9.6 (*6*, *19*). In the crystal structure of the product complex of SaDHNA, K100 is hydrogen bonded to the carboxyl group of E22, the hydroxyl group of Y54, and the water molecule that serves as a general acid. It probably has a normal p$K_a$ of ~10, which matches closely with the optimal pH of the enzymatic reaction. On the other hand, the carboxyl group of E22 is hydrogen bonded to the hydroxyl of HP, the main chain NH group of L19, and the side chain amide of Q27. The p$K_a$ of E22 is unlikely to be higher than 4.5, the p$K_a$ of model peptides, which is too far from the optimal pH of the enzymatic reaction. Another possibility is that the protonated amino group of K100 serves a general acid and donates its proton via the water molecule to N5 of DHNP and the carboxyl group of E22 serves as a general base to deprotonate the 2′-OH group of DHNP. The pH profiles of the wild-type and mutant enzymes may help to resolve this issue. Unfortunately, we were unable to obtain the pH profiles for the mutants because of their low activities.

While E74 of SaDHNA and the corresponding residue in EcDHNA (E73) play a common role in the enzymatic reaction, namely, in the binding of the substrate, the roles of E22 and K100 of SaDHNA are slightly different from those of corresponding residues E21 and K98 in EcDHNA. Both E22 and K100 of SaDHNA are involved in catalysis, but neither contributes to the binding of the substrate. On the other hand, in addition to their roles in catalysis, both E21 and K98 are also involved in the binding of the substrate. The different biochemical properties between SaDHNA and EcDHNA revealed by the previous study of the wild-type enzymes and this site-directed mutagenesis study suggest that it is possible to develop specific inhibitors for these two enzymes.

## ACKNOWLEDGMENT

We are grateful to Mr. Joseph Leykam for expert assistance in the HPLC analysis.

## REFERENCES

1. Walsh, C. (2003) Where will new antibiotics come from? *Nat. Rev. Microbiol. 1*, 65−70.
2. Bermingham, A., and Derrick, J. P. (2002) The folic acid biosynthesis pathway in bacteria: Evaluation of potential for antibacterial drug discovery, *BioEssays 24*, 637−648.
3. Kompis, I. M., Islam, K., and Then, R. L. (2005) DNA and RNA synthesis: Antifolates, *Chem. Rev. 105*, 593−620.
4. Blakley, R. L., and Benkovic, S. J. (1984) in *Folates and pterins*, John Wiley & Sons, New York.
5. Sanders, W. J., Nienaber, V. L., Lerner, C. G., McCall, J. O., Merrick, S. M., Swanson, S. J., Harlan, J. E., Stoll, V. S., Stamper, G. F., Betz, S. F., Condroski, K. R., Meadows, R. P., Severin, J. M., Walter, K. A., Magdalinos, P., Jakob, C. G., Wagner, R., and Beutel, B. A. (2004) Discovery of potent inhibitors of dihydroneopterin aldolase using crystalead high-throughput X-ray crystallographic screening and structure-directed lead optimization, *J. Med. Chem. 47*, 1709−1718.
6. Mathis, J. B., and Brown, G. M. (1970) The biosynthesis of folic acid XI. Purification and properties of dihydroneopterin aldolase, *J. Biol. Chem. 245*, 3015−3025.
7. Horecker, B. L., Tsolas, O., and Lai, C.-Y. (1975) Aldolases, in *The enzymes* (Boyer, P. D., Ed.) pp 213−258, Academic Press, San Diego.
8. Allen, K. N. (1998) Reactions of enzyme-derived enamines, in *Comprehensive biological catalysis* (Sinnott, M., Ed.) pp 135−172, Academic Press, San Diego.
9. Hauβmann, C., Rohdich, F., Schmidt, E., Bacher, A., and Richter, F. (1998) Biosynthesis of pteridines in *Escherichia coli*: Structural

and mechanistic similarity of dihydroneopterin-triphosphate epimerase and dihydroneopterin aldolase, *J. Biol. Chem. 273*, 17418−17424.
10. Hennig, M., D'Arcy, A., Hampele, I. C., Page, M. G. P., Oefner, C., and Dale, G. E. (1998) Crystal structure and reaction mechanism of 7,8-dihydroneopterin aldolase from *Staphylococcus aureus*, *Nat. Struct. Biol. 5*, 357−362.
11. Goulding, C. W., Apostol, M. I., Sawaya, M. R., Phillips, M., Parseghian, A., and Eisenberg, D. (2005) Regulation by oligomerization in a mycobacterial folate biosynthetic enzyme, *J. Mol. Biol. 349*, 61−72.
12. Bauer, S., Schott, A. K., Illarionova, V., Bacher, A., Huber, R., and Fischer, M. (2004) Biosynthesis of tetrahydrofolate in plants: Crystal structure of 7,8-dihydroneopterin aldolase from *Arabidopsis thaliana* reveals a novel adolase class, *J. Mol. Biol. 339*, 967−979.
13. Wang, Y., Scherperel, G., Roberts, K. D., Jones, A. D., Reid, G. E., and Yan, H. (2006) A point mutation converts dihydroneopterin aldolase to a cofactor-independent oxygenase, *J. Am. Chem. Soc. 128*, 13216−13223.
14. Li, Y., Gong, Y., Shi, G., Blaszczyk, J., Ji, X., and Yan, H. (2002) Chemical transformation is not rate-limiting in the reaction catalyzed by *Escherichia coli* 6-hydroxymethyl-7,8-dihydropterin pyrophosphokinase, *Biochemistry 41*, 8777−8783.
15. Shi, G., Gong, Y., Savchenko, A., Zeikus, J. G., Xiao, B., Ji, X., and Yan, H. (2000) Dissecting the nucleotide binding properties of *Escherichia coli* 6-hydroxymethyl-7,8-dihydropterin pyrophosphokinase with fluorescent 3′(2)′-O-anthraniloyladenosine 5′-triphosphate, *Biochim. Biophys. Acta 1478*, 289−299.
16. Schulz, A. R. (1994) *Enzyme kinetics: From disease to multienzyme systems*, Cambridge University Press, New York.
17. Howell, E. E., Villafranca, J. E., Warren, M. S., Oatley, S. J., and Kraut, J. (1986) Functional role of aspartic acid-27 in dihydrofolate-reductase revealed by mutagenesis, *Science 231*, 1123−1128.
18. Birdsall, B., Casarotto, M. G., Cheung, H. T. A., Basran, J., Roberts, G. C. K., and Feeney, J. (1997) The influence of aspartate 26 on the tautomeric forms of folate bound to *Lactobacillus casei* dihydrofolate reductase, *FEBS Lett. 402*, 157−161.
19. Mathis, J. B., and Brown, G. M. (1980) Dihydroneopterin aldolase from *Escherichia coli*, *Methods Enzymol. 66*, 556−560.
20. Kraulis, P. J. (1991) Molscript: A program to produce both detailed and schematic plots of protein structures, *J. Appl. Crystallogr. 24*, 946−950.
21. Bacon, D. J., and Anderson, W. F. (1988) A fast algorithm for rendering space-filling molecule pictures, *J. Mol. Graphics 6*, 219−220.
22. Merritt, E. A., and Bacon, D. J. (1997) Raster3d: Photorealistic molecular graphics, *Methods Enzymol. 277*, 505−524.

BI060949J